Waste Management 102 (2020) 21–29

Contents lists available at ScienceDirect

Waste Management

journal homepage: www.elsevier.com/locate/wasman

Waste tires pyrolysis kinetics and reaction mechanisms explained by TGA and Py-GC/MS under kinetically-controlled regime

Tamara Menares [a,b], Jorge Herrera [a], Romina Romero [b], Paula Osorio [a], Luis E. Arteaga-Pérez [a,*]

[a] Laboratory of Thermal and Catalytic Processes (LPTC), Department of Wood Engineering, University of Bío-Bío, Concepción, Chile
[b] Technological Development Unit, Universidad de Concepción, Coronel, Chile

ARTICLE INFO

Article history:
Received 16 July 2019
Revised 9 October 2019
Accepted 12 October 2019

Keywords:
Waste tires
Pyrolysis
Kinetics
Py-GC/MS
Reaction mechanism

ABSTRACT

The fast pyrolysis of waste tires (WTs) is studied by quasi-isothermal thermogravimetric (TGA) analysis, kinetic modelling and an analytical pyrolyzer coupled with gas chromatography/mass spectrometry (Py-GC/MS). The TGA demonstrated that the WTs pyrolysis is ruled by devolatilization/condensation and depropagation reactions, up to 482 °C. At higher temperatures, the cyclization and aromatization of primary products take place to form mostly monoaromatics. Py-GC/MS experiments were performed under kinetic regime according to the thermal map established by the ratio between Bioś (31.25) and Py-numbers ($7.7{\cdot}10^6$). Limonene (51%) and isoprene (20.5%) were the major compounds detected at temperatures below 435 °C, while above 600 °C limonene was converted to mono-aromatics (S_{BTX} = 28.7%). The approach to equilibrium of Diels-Alder reaction demonstrated that there is an equilibrium-ruled behavior between isoprene and limonene, particularly at T > 600 °C. The E_a values calculated by the Starinḱs model ranged from 101.5 to 176.7 kJ/mol, while for model-based kinetics it was 152.7 kJ/kmol. The integration of TGA, kinetic modelling and Py-GC/MS provided insights into pyrolysis reaction mechanism.

1. Introduction

The continuous growth of world population and the changes in the life standards are the main causes for the depletion of natural resources (i.e., petroleum, minerals, etc). Moreover, the consumption-oriented development model implemented at global scale, have produced irreversible damages to ecosystems, water depletion and atmospheric contamination. Therefore, the shift from a fossil-based society to a renewable-based one, is a challenge that the scientific community is facing nowadays (Palmeros Parada et al., 2017). Nevertheless, this change cannot be focused only in replacing the oil by biomass, but also, by producing a breakpoint in the value chain of materials. In this sense, there is a pressing need for migrating from the linear model of *production → consumption → disposal* to a circular strategy, which allows using residues as feedstock for new processes. In this endeavor, a plethora of strategies for recycling and valorizing residues are being studied under the concept of circular economy (Hassan et al., 2019).

The world market for light vehicles is increasing steeply. In 2019 the global production of cars will reach 95 millions of units, with a prospective growth of 110 millions of units by 2025 (Wall, 2019). Accordingly, the demand for tires (ref. 2.9 billions in 2017) will also increase, imposing a major challenge to reuse or dispose this complex material after use. Particularly in Chile, around 140 000 tons of waste tires (WTs) are generated in a yearly basis. According to a recent report, only a 17% of the waste tires in Chile are reused or recycled, the rest is accumulated in non-controlled areas affecting the environment (Portal, 2019). These facts have contributed to an incipient interest for developing processes and recycling strategies for WTs, in order to reduce their effects to the environment and to take advantage of them as feedstock for marketable products.

Thermochemical transformations are the most common processes used for the valorization or disposal of WTs. Moreover, incineration and combustion of WTs are attractive solutions for the production of heat and power in conventional coal-based plants (Oboirien and North, 2017; Singh et al., 2009). However, these *destructive* processes do not allow obtaining more valuable products from the different fractions of the tires (rubber, metal, carbon black). Instead, the fast pyrolysis has emerged as a conscious solution for the valorization of the rubber and to recover the carbon black and metals from used tires (Martínez et al., 2013).

The fast pyrolysis of WTs is a thermochemical degradation occurring at high temperatures (typically 400–800 °C) in an oxygen-free or oxygen-depleted atmosphere. The WTs pyrolysis products includes a liquid (oil), which can be used directly as boiler

* Corresponding author.
E-mail address: larteaga@ubiobio.cl (L.E. Arteaga-Pérez).

https://doi.org/10.1016/j.wasman.2019.10.027
0956-053X/

fuel or as feedstock for the extraction of more valuable compounds such as limonene, benzene, toluene and xylene (BTX). Additionally, a gas and a solid are also obtained, being the first used to fulfill the energy requirements of the pyrolysis process. While the solid product, -also known as recovery carbon black (rCB)-, can be used for producing activated carbon, as additive for improved asphaltic and concrete mixtures, and as a substitute of Carbon Black (Dimpe et al., 2018; Lo Presti, 2013; Martínez et al., 2019; Trubetskaya et al., 2019). It is widely accepted that the yield and composition of the pyrolysis products heavily depends on the process temperature (controlling the kinetics), particle sizes (affecting transport limitations) and heat transfer mechanisms (i.e., reactor design) (Oyedun et al., 2012). Ucar et al. (2005) reported on the effect of the polymers types and the temperature on the composition of WTs-derived oil. They witnessed that at high temperatures the content of paraffins in the oil increased; while the product distribution did not change in a high extent. Nevertheless, few information on the kinetics or reaction mechanisms taking place during pyrolysis was provided in that work.

In an endeavor for valorizing waste tires Zhang et al. (2008) studied the vacuum pyrolysis of tire granules and demonstrated that dl-limonene production was highly sensitive to temperature, being promoted at T < 500 °C. Based on their experimental observations Zhang et al. (2008) suggested that dl-limonene is formed by β-scission of poliestyrene with later cyclization and, parallelly via Diels-Alder coupling of two isoprene monomers. Although a comprehensive analysis based on products distribution was presented, Zhang et al. (2008) did not provide kinetic predictions based on their observations; neither did they discuss on the regime (thermally or kinetic-controlled) at which the experiments were carried out. In a more recent paper, Xu et al. (2018), studied the pyrolysis of bicycle tires by coupling thermogravimetric analysis (TGA) with Fourier transform infrared spectroscopy (FTIR). They observed that the different polymers in the WTs decompose by a series of condensation, polymerization, depropagation, hydrogenation and aromatization reactions, with a noticeable influence of temperature. In this paper, Xu et al. (2018) followed the steps of Zhang et al. (2008) and, based in a TGA-FTIR analysis, they confirmed that dl-limonene is formed according to the above mentioned reactions. Nevertheless, Xu et al. (2018) did not mentioned the kinetic implications of their findings and how the thermal mapping of their pyrolytic experiments influenced the results. This last issue was addressed by Paulsen et al. (2013) who demonstrated that sample size is a key descriptor for products yields during cellulose pyrolysis due to the effect that heat transfer exert on the experimental results. Accordingly, Paulsen et al. (2013) provided the definition of a pyrolysis reaction-transport map, which can be used for comparing heat transfer and reaction time scales in order to develop pyrolysis experiments under transport-free limitations. However, to the best of our knowledge, this criteria has not been applied to WTs pyrolysis, thus most of the results are specific for the scale at which the experiments are performed (Arabiourrutia et al., 2019, 2007). In fact, the kinetics of WTs pyrolysis have been extensively studied, from the pioneering works of Kim et al. (1995); Williams and Besler (1995), until the recently publications of Arabiourrutia et al. (2019); Chen et al. (2019). Accordingly, there is a plethora of kinetic data for describing the thermal decomposition of WTs and its constituent polymers (natural rubber, butadiene rubber and styrene-butadiene rubber) using TGA. Nevertheless, there is a consensus in concluding that the reliability of the kinetic data for WTs pyrolysis, heavily relies on the experimental conditions, due to the data is usually gathered under temperature-controlled experiments. Therefore, it is of paramount important studying the WTs pyrolysis under kinetic controlled conditions, at different temperatures and, using integrated modelling approaches. In fact, these are the major contributions of the present paper, where kinetic predictions are integrated to Py-GC/MS experiments in order to understand the major steps in the WTs pyrolysis reaction map.

Efforts for elucidating the WTs pyrolysis mechanisms and to find the optimal operation conditions *en route* to apply this technology at larger scale are being carried out. Han et al. (2018) studied the pyrolysis mechanisms by coupling TGA-MS and by studying the functional groups in the residue char through FTIR. They suggested that the process proceed via a four stages mechanism involving: (i) the dehydration and plasticizers decomposition, (ii) conversion of natural rubber, (iii) decomposition of synthetic rubbers and (iv) final conversion. Nevertheless, these authors did not provide any data related to the process kinetics, neither about the possible reaction map describing the WTs pyrolysis. This gap was fulfilled by Xu et al. (2018) who proposed a three reaction scheme governed at higher temperatures (<700 °C) by the formation of aromatics from limonene and styrene. However, no kinetic or equilibrium calculations confirmed the reaction routes proposed by Xu et al. (2018). Similarly, Mkhize et al. (2016) proposed a mechanism to explain the formation of limonene starting from isoprene monomers and including scission/aromatization reactions. The later was addressed in detail by Ding et al. (2015) in a Py-GC/MS system and, they proposed that limonene is decomposed in several stages to form radicals, aromatics and gases at 500 °C and above 600 °C, respectively. Beside aromatics and heavier compounds, gases are an important fraction of pyrolysis products which has been studied in less extent. In this sense, Wei et al. (2019) have recently reported on the reaction routes leading to gases formation during WTs pyrolysis. They supported the study on reaction molecular dynamic simulations and TGA-FTIR experiments. Nevertheless, this study was restricted to gas formation, hence the polymeric decomposition phases and aromatics formation was out of the scope.

Considering the above-discussed, the WTs pyrolysis is studied here by coupling TGA and Py-GC/MS analyses with kinetic modelling. Major chemical transformations taking place during the process and thermal regime of the Py-GC/MS are assessed together in order to guarantee kinetic control during experiments. The WTs are characterized here for elemental and proximate analyses, trace elements quantification via inductively coupled plasma optical emission spectrometry (ICP-OES), attenuated total reflectance Fourier transform infrared spectroscopy (FTIR-ATR) and, using regular and quasi-isothermal TGA experiments.

2. Materials and methods

The polymeric fraction of automobile waste tires (denoted as WT) was used here. Samples were obtained from a local enterprise (Polambiente S.A.), which provided the tires residues as granules. After drying, the granules were crushed and sieved (Gilson ASTME11) to different particle sizes (e.g., 75–180 μm, 180–300 μm and 300–500 μm) and stored in hermetic plastic bags.

2.1. Compositional analysis

The proximate composition of the WTs was studied in a muffle furnace (Thermo Scientific F6020C) according to the ASTM D3172 Standard, while the ultimate composition was determined in a Leco CHNS 628 elemental analyzer. Furthermore, the trace inorganic elements were quantified by inductively coupled plasma optical emission spectrometry (ICP-OES) using a PerkinElmer Optima 7000 DV ICP-OES series instrument. Analysis of the solid samples was performed via acid digestion according to the standard ISO 9028:2006 (Rubber – Dissolution by acid digestion). Typically, 250 mg of sample (<75 μm) were placed inside Teflon

vessels and mixed with 2 mL of HNO_3 (65%, Merck, Germany). Thereafter, the mixture was heated up at 8 °C/min until 200 °C (20 min holding time), in a microwave oven (MARS 6 CEM, USA). Measurements of the resulting digestate were done by triplicate in order to verify replicability of the results as the relative standard deviation (%RSD) of independent samples. The measurement of the trace elements is of high importance in order to discard important catalytic effects of metal species during pyrolysis.

Finally, the HHV of the material was estimated by the Boiés (Han et al., 2017) correlation, for polymers and biomass.

2.2. Fourier transformed spectroscopy (FT-IR)

The functional groups in the WTs samples were studied via FT-IR using spectra recorded at room temperature and ambient pressure in a BRUKER ALPHA FT-IR spectrometer equipped with a platinum attenuated total reflection (ATR) single-reflection module. The spectra of the pre-dried samples were averaged from 32 scans using a resolution of 2 cm^{-1} over the mid-IR range (4000–400 cm^{-1}). Data was analyzed using OPUS 7.0.129 software.

2.3. Thermogravimetric analysis (TGA-DTG)

The weight loss and differential thermal analysis (DTA) as a function of temperature were recorded using a thermobalance (Netzsch, model STA 409 PC) from 20 °C to 650 °C using the quasi-isothermal method reported by Miranda et al. (2006). Although this method needs for longer times than a regular TGA assay, it allows identifying the decomposition phases of the polymer with an improved signal/noise ratio. Moreover, the data gathered from this experiment can be used along with iso-conversional kinetic experiments, to support the WTs understanding. In a typical experiment, 20 mg of sample (ground and sieved to 75–180 μm) were placed in an alumina crucible and heated under a N_2 flow (50 mL/min). Temperature cycles were of 20–25 min of heating at 20 °C/min and 20 min of dwell time at the specific temperature, yielding a total of 12 isothermal stages. Moreover, a series of regular TGA analysis were performed at continuous heating rates (i.e., 5 °C/min, 10 °C/min, 20 °C/min and 30 °C/min) and using the same carrier gas N_2 (50 mL/min). The buoyancy effect during TGA experiments was avoided by subtracting a blank baseline curve from each experiment.

2.3.1. WTs thermal decomposition kinetics

The kinetics for the decomposition of WTs was approached by two methods: a model-based kinetics and a model-free kinetics (Starink, 2003). The model-based kinetics follows the same logic to that reported elsewhere (Danon et al., 2015). First, a power law representation is assumed to obtain the deconvolution of the total conversion function:

$$d\alpha_i/dt = k_i \cdot (1-\alpha_i)^{n_i} \quad (1)$$

The kinetic constant of the i-th devolatilization reaction can be represented as an Arrhenius model, the Eq. (1) results in the following:

$$d\alpha_i/dt = A_i \times exp(-Ea_i/RT)(1-\alpha_i)^{n_i} \quad (2)$$

It is assumed that each devolatilization reaction is independent and, the overall change in the conversion is the weighted sum of individual reactions; thus, total conversion function is written as follows:

$$d\alpha/dt = \sum_{i=1}^{3} w_i \times (d\alpha_i/dt), i = NR, BR, SBR \quad (3)$$

Then a system of ODEs is formed, depending on the number of devolatilization reactions and, considering that $\sum_{i=1}^{3} w_i = 1$. Finally, the kinetic triplet (A_i, Ea_i, and n_i) is calculated by minimizing the square sum error (Eq. (4)) between measured and modeled data:

$$error = \sum_{t_0}^{t_f} \left[(d\alpha/dt)_{exp} - (d\alpha/dt)_{mod} \right]^2 \quad (4)$$

The global activation energy and pre-exponential factor for the WTs pyrolysis are obtained by correlating the TGA in the reaction zone (200–505 °C). To that aim the Eq. (2) was linearized:

$$ln(d\alpha/dt) = ln(A) - Ea/RT + ln(1-\alpha)^n \quad (5)$$

Then, the Ea and A are obtained by plotting $ln\left[(d\alpha/dt)/(1-\alpha)^n\right]$ versus $(-1/T)$.

Here α is the mass loss conversion, Ea is the activation energy (kJ/mol), A is the preexponential factor, R is the universal gas constant (kJ/kmol/K), n is the reaction order. Subscripts *exp* and *mod* refers to experimental data and model results, respectively.

Despite the model-based kinetics is a good approximation to the kinetics of tire pyrolysis, it represent an oversimplification of the process by considering individual reaction steps. Therefore, here the model-free approach of Starink (Eq. (6)) is used. This model integrates the *iso*-conversional methods of Flynn-Wall-Ozawa (FWO) and Kissinger-Akira-Sunose (KAS) into a single expression (Starink, 1996):

$$Ln\left(\beta/T^{1.8}\right) = C_s - 1.0037(Ea/RT) \quad (6)$$

Starink's activation energy is obtained from the slope of ln ($\beta/T^{1.8}$) against 1/T whilst Cs is a constant independent of β and T. This method has been applied in several kinetic studies, and it has been reported to be at least an order of magnitude more accurate than the FWO and KAS approaches (Starink, 2003).

2.4. Pyrolysis coupled to mass spectrometry (Py-GC/MS)

The WTs samples between 75 and 180 μm were used for Py-GC/MS, in order to reduce transport limitations during reaction. Thereafter, 50 mg of the mixture were placed into a sample cup (Frontier Laboratories Eco-cup, 80 μL) and dropped into the pre-heated furnace using an auto-shot sampler (heating rate 2000 °C/s). Pyrolysis was performed between 350 and 800 °C.

The Py-GC/MS experiments were performed in a micropyrolysis system (EGA/PY-3030D, Frontier Laboratories) interfaced with a gas chromatograph (GC-2010 Plus, Shimadzu) equipped with a single quadrupole mass spectrometry detector (QP 2010 Ultra, Shimadzu). The interface line was kept at 300 °C in all the experiments and a constant gas flow (50 mL/min) of He (pure He, 99.999%, Airliquide, Chile) was used to carry the volatiles out from the pyrolysis zone. The pyrolysis products (1:50 split ratio) were separated in a BP10 capillary column (30 m × 0.25 mm) with 14% Cyanopropylphenyl polysiloxane as stationary phase and were analyzed in a MS detector (70 eV ionization) within a m/z range of 2–800. The identification of compounds in the Py-GC/MS spectra was carried out by considering a minimum cut-off score of 80%, with respect to the National Institute of Standards and Technology (NIST) mass spectral database.

2.4.1. Data processing

The detection capability of the GC technique is limited by the volatility of the compounds being analyzed and to the response of the detector to specific species. That's why the Py-GC/MS cannot provide an accurately quantitative analysis of the compounds formed during WTs pyrolysis. Nevertheless, a linear proportionality between the chromatographic peaks area corresponding to a

particular compound and its relative concentration could be established. Based on this principle, the selectivity to specific specie is estimated by the ratio between the chromatographic peak area of a ith-compound ($PArea_i$) and the sum of total detected peak areas ($\Sigma PArea_i$) (Eq. (7)).

$$S_i = 100 \times \left(PArea_i / \sum_{i=1}^{n} PArea_i \right) \quad (7)$$

Owing to that, the following criteria were defined to discuss the effect of operational parameters:

Relative selectivity among functional groups:

The factor $\xi_{a\text{-}b}$ (Eq. (8)) is used to quantify the relative formation of interest compounds.

$$\xi_{a-b} = (S_a/S_b)a, b \quad : produced\ \ compounds\ \ i.e.\ \ alkenes, aromatics, limonene, etc. \quad (8)$$

3. Results and discussion

3.1. Compositional characterization and FT-IR

Proximate and ultimate analyses allows identifying the potentialities of WTs to be used for pyrolysis or combustion processes. Results (Table 1) evidenced that the fast pyrolysis (mostly devolatilization/condensation reactions) of this material is feasible, considering its high content of volatile matter (58.8%). The fixed carbon (non-volatile) and ash fractions of WTs, includes the carbon black and inorganics (different to steel), respectively. The ICP-OES analysis allows confirming the presence of transition and alkali metals in the WTs.

The results are in good agreement with those previously reported for WTs collected from similar sources, for which volatile matter ranged between 58 and 66% and fixed carbon between 27.5 and 32% (Akkouche et al., 2017; Li et al., 2016; Miandad et al., 2018; Ucar et al., 2005). Nevertheless, the ash content found here is higher than in those reports (4.2–5.4%), presumably by the differences in the process for separating the rubber from the tires (here is by abrasion). Based on its high carbon content, the WTs is an attractive source for energy production, either by direct combustion or as feedstock for obtaining liquid fuels. In fact, the HHV estimated by Boiés correlation was similar to that of a bituminous coal, used for coal-fueled boilers (Akkouche et al., 2017; Miandad et al., 2018).

The FTIR-ATR spectrum shows characteristic bands at 2912 and 2838 cm^{-1} which are typically attributed to —CH— asymmetric stretching of —CH_3 and —CH_2— chemical groups and, to the —C—H symmetric stretching of the same groups. These vibrational signals are common in several polymers; thus they cannot be considered a footprint for NR, SBR or BR. Nevertheless, according to the ASTM D3667 standard, the additional signals at 1372 cm^{-1} (methyl radical) and 887 cm^{-1} confirmed the presence of NR. The same standard (ASTM D3667), suggest that the bands found between 960 and 985 cm^{-1} are attributed to the vibration of C—H in butadiene (BR) double bonds, while signals at 1421, 1548 and 701 cm^{-1} are typical of SBR spectrum and, indicates the C—C, C—H and C—N stretching, respectively (Khan et al., 2017; Nunes et al., 2018). The weak signals between 600 and 520 cm^{-1} allows confirming the presence of C—S bonds, which was also confirmed by elemental analysis (See Fig. S1 in Supplementary Material). The results from the FTIR-ATR and compositional analyses suggest the presence of NR, BR and SBR in the WTs. However, some of the IR signals can be associated to the tires additives; thus, they could affect the accuracy of the FTIR-based predictions.

3.2. Thermogravimetric analysis and kinetics

3.2.1. TGA-DTG and DTA

The TGA/DTG results obtained from the quasi-isothermal approach and for typical thermogravimetric experiments are presented in Figs. 1 and 2, respectively. The quasi-isothermal DTG curve shows 8 decomposition steps which can be explained by the different reaction phases taking place during WTs pyrolysis. The first two steps, occurring between 100 °C and 200 °C, are associated to the devolatilization of plasticizers and corresponds to a negligible weight loss (<2% in the TGA). Above 230 °C and until 300 °C occurs the third and four decomposition steps, corresponding to 11% weight loss to the total TGA and it is attributed to the formation of radicals from NR and BR. Thereafter, there are three pronounced DTG peaks (steps 5–7) corresponding to the most important weight loss (21%). In fact, major reactions occurring in this temperature range (330–420 °C) are depolymerization (forming mono/-dimers) and devolatilization/condensation reactions of NR and SBR (Danon and Gorgens, 2015). Finally, the quasi-isothermal DTG shows a wide peak at 435 °C, which relates to the scission of C—C to form C=C, here between 420 and 505 °C (8% wt. loss). The completion of the pyrolysis process was around 510 °C, with a final residue of 37% in the TGA, which coincides with the fixed carbon and ash contents calculated by proximate analysis. These results are similar to that previously reported in literature (Danon et al., 2015; Leung and Wang, 1999; Mkhize et al., 2016).

The quasi-isothermal approach allows confirming the presence of the NR, BR and SBR in the WTs and to establish temperature limits for the different decomposition phases, similar to that widely reported for regular TGA experiments (Seidelt et al., 2006). The later could be coupled to kinetic estimations to better understand the WTs pyrolysis and the energy balance controlling the reaction mechanism.

In order to confirm the quasi-isothermal results and to gather data for performing kinetic analysis, several TGA experiments were carried out. The Table 2 and Fig. 2 shows the TGA, DTG and DTA results at β = 20 °C/min, for which the TGA ended at 505 °C with a final 38% solid residue, which confirms the results obtained during the quasi-isothermal approach under the same β. The DTG

Table 1
Compositional analysis of WTs.

Proximate Analysis (wt.%)$_{a.r.}$		Ultimate Analysis (wt.%)$_{d.b.}$		Alkali Metals (mg/kg) $_{d.b.}$	
Moisture content (MC)	1.2	C	79.54 ± 0.17	Al	1352
Volatile matter (VM)	58.76	H	7.33 ± 0.03	Ca	1152
Fixed carbon (FC)	30.15	N	0.47 ± 0.03	Fe	1117
Ash	9.89	S	1.48 ± 0.06	K	509
HHV* (MJ/kg)$_{d.b.}$	36.55	O**	1.29	Na	508

* HHV (MJ/kg) = 35.2C + 116.2H + 6.3 N + 10.5S − 11.1O, where C, H, O, S, N are fractional elemental composition of carbon, hydrogen and oxygen, respectively (Han et al., 2017).

** Oxygen is calculated by difference from O = 100 − C% − N% − H% − S% − ASH%.

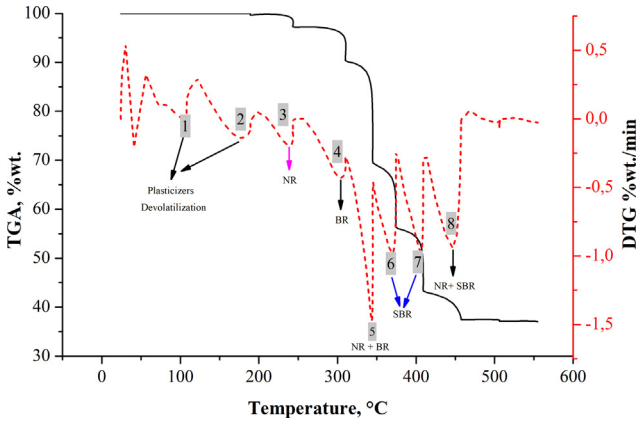

Fig. 1. Quasi-isothermal TGA and DTG curves of WTs. Identification of DTGs peaks corresponding to tire constituents decomposition. β = 20 °C/min, 20 min dwell time.

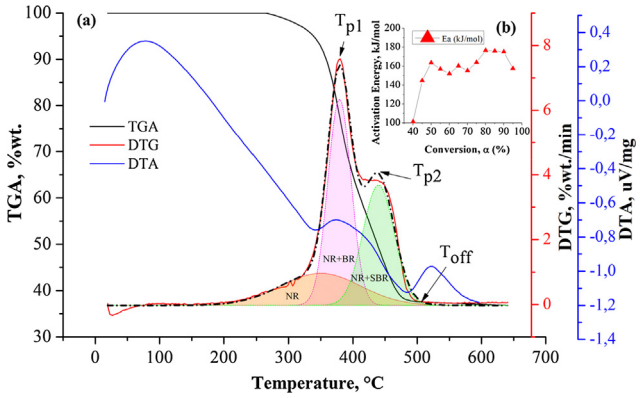

Fig. 2. TGA, DTA and Activation energy for WT thermal decomposition. Filled areas represents NR, SBR, BR decomposition. Dashed black line is the model-predicted DTG data.

curve presented a main devolatilization peak (T_{p1}) around 379 °C with a shoulder (T_{p2}) at 432 °C, both typical of polyisoprene rubbers (Danon and Gorgens, 2015). In fact, the devolatilization/condensation reactions taking place at lower temperatures are prone to form radicals which subsequently form condensation products. Finally, these condensation products undergo fragmentation and rearrangements to form pyrolysis products (Mkhize et al., 2016; Xu et al., 2018; Zhang et al., 2008). These results are in line to that reported by Danon et al. (2015); Senneca et al. (1999) which reported a maximum devolatilization peak at temperatures between 366 °C and 396 °C, depending on the heating rate used for TGA. Moreover, Danon et al. (2015) stated that the first devolatilization peak is associated to the decomposition to the polyisoprene and, in less extent, to SBR. Therefore, is at these lower temperatures where some alkenes (e.g., isoprene and limonene) are abundant in the pyrolysis vapors (Mkhize et al., 2016; Xu et al., 2018).

From the enthalpy viewpoint there are some interesting facts; for example, the DTA curve shows two negative peaks representing endothermic processes, presumably during the devolatilization of tire constituents. This behavior could be associated to the C—C and C=C bonds breakage (ca. 334–606 kJ/mol) for the formation of radicals (Zhang et al., 2008). In the final section of the DTA (above 482 °C) there is a clear exothermic peak, which is attributed to the rearrangement reactions (i.e. Diels-Alder cyclization and depolymerization) occurring after devolatilization. The exothermicity is expected to be more important at higher temperatures, where the cyclization and other reactions leading to the formation of aromatics take place (Xu et al., 2018).

According to the above discussed, the thermal decomposition of the WTs can be described by devolatilization/condensation reactions with subsequent conversion of radicals, mono/-dimers to char, volatiles and gas. Moreover, the process is balanced between endothermic and exothermic reactions, depending on the temperatures and on the bond energies of the molecules being converted or formed during the pyrolysis. These results are in good agreement with that previously reported in the literature (Akkouche et al., 2017; Danon and Gorgens, 2015; Leung and Wang, 1999).

3.2.2. Kinetics modelling

The kinetics of the waste tire pyrolysis have been extensively studied. Since the pioneering works of Kim et al. (1995); Williams and Besler. (1995), there is consensus about there are no single parameters or models with the capacity to give a generalized description of the tire pyrolysis. Instead, the kinetics and the reaction mechanisms heavily relies on the composition of the WTs, particularly on the fraction of NR, SBR and BR and on the conditions at which the TGA experiments are carried out (particle sizes and β). Accordingly, there is a plethora of activation energies and rate laws to describe the kinetics of WTs based on milligram and gram-scale data. Here, the activation energies for a model-based and a model-free kinetic approaches are provided.

The peak differentiation for the DTG (colored areas in Fig. 2) was used to obtain the model-based kinetic parameters. The differentiation was approached by three Gaussian functions, attributed to the decomposition of NR, BR and SBR, respectively. These functions were then adjusted by the least squares method using as the model parameters, the kinetic triplet (Ea, A and n) and comparing the experimental data to that predicted by the model (Table 2). The simulation of the DTG curve described by the sum of the three Gaussians derived from the model-based kinetics shows a very good agreement to the experimental data ($R^2 > 0.98$). Moreover, the result for a global activation energy (152.7 ± 3 kJ/mol)

Table 2
TGA parameters and apparent activation energies from kinetic modelling.

Materials	T_{p1} (°C)	T_{p2} (°C)	T_{off} (°C)	**Model-based** E_a (kJ/mol) log (A) (s^{-1})	**Model-Free** Ea (kJ/mol)		
					E_{amin}	E_{amax}	Models
WTs (this paper)	379 ± 4	432 ± 6	505 ± 3	152.7 ± 3 3.5 ± 0.03	101.5 ± 2	176.7 ± 2	Starinks
WTs (Dahwi) (Danon and Gorgens, 2015)	375	429	515	246	221	239	Friedman
NR, BR, SBR (Danon et al., 2015)	370	460	500	N/A	200	440	Friedman
WTs (Leung and Wang, 1999)	379	458	500	52–164	N/A	N/A	N/A
WTs (Williams and Besler, 1995)	385	420	505	132.7–134.7	N/A	N/A	N/A
WTs (Arabiourrutia et al., 2019)	N/A	N/A	N/A	70–122	N/A	N/A	N/A
WTs (Cheung et al., 2011)	403	N/A	500	69–128	N/A	N/A	N/A
WTs (Khiari et al., 2018)	N/A	N/A	480	61–129	N/A	N/A	N/A

coincides with those reported by several authors working with WTs (Arabiourrutia et al., 2019; Cheung et al., 2011; Leung and Wang, 1999; Williams and Besler, 1995).

Although a global activation energy is a good approach to the process kinetics; describing the different decomposition phases of a WTs (demonstrated in the TGA) by a single kinetic model is an oversimplification of the process. Instead, the activation energy distribution function calculated from the Starinḱs method is provided (Fig. 2b). The results for the model-free E_a are in good agreement with the results obtained by Williams and Besler (1995), who demonstrated that E_a for the conversion of the individual constituents present higher values (195–223 kJ/mol at 20 °C/min heating rate) than those found for WTs. These results were recently corroborated by Danon et al. (2015) who combined model-based and model-free kinetics approaches to study the devolatilization of rubber and tires.

The E_a values calculated by the Starinḱs model ranged from 101.5 to 176.7 kJ/mol, and the E_a vs α profile allows identifying two major regions. The first (between 358 °C and 382 °C) is probably associated to the devolatilization/condensation of NR and SBR. Mkhize et al. (2016) suggested that in this region the allylic polyisoprene radicals undergoes depropagation and intramolecular cyclization-scission to form isoprene and limonene. The second region between 387 and 433 °C could be associated to the scission and dehydrogenation of the SBR leading to the formation of styrene and butadiene monomers.

3.3. Micro-pyrolysis coupled to mass spectrometry

The pyrolysis of WTs is a process which features an interesting behavior regarding the products distribution and composition. In this sense, the particle sizes, sample mass, heating rate, furnace design and most importantly the reaction temperature plays a determinant role by controlling transport limitations and reaction kinetics (Carrier et al., 2017; Paulsen et al., 2013). As evidenced during the TGA experiments, the WTs is converted through devolatilization/condensation reactions at lower temperatures (around 400 °C); thereafter undergoes a series of reaction steps leading to the formation of monomeric compounds (i.e. isoprene) and their derivatives (limonene, styrene). Here, several Py-GC/MS experiments were carried out, to correlate the TGA data and kinetic findings, with the possible reaction routes occurring during WTs fast pyrolysis.

3.3.1. Compounds identification

Most abundant compounds identified during non-catalytic pyrolysis of WTs at temperatures between 400 and 800 °C are: *gases* (e.g., alkanes, alkenes, CO_x and H_2), *cyclic hydrocarbons* formed from intra-molecular cyclization and depropagation of natural rubber (Cyclo-butene, cyclo-propane, limonene and isoprene) and *aromatics* (xylene, benzene, styrene). The aromatics are formed after extensive conversion of the cyclic products by aromatization and hydrogenation reactions (Arabiourrutia et al., 2007; Ding et al., 2016; Ucar et al., 2005). The most important products identified during Py-GC/MS are presented in Fig. S2 along with a complete list of detected compounds (Table S1).

Two intense peaks are identified at 4.8 and 22.3 min, respectively, which corresponds to a monomer (isoprene) of NR and a dimmer (limonene), respectively. The combined peak-based selectivity of these two compounds is nearly 80% below 600 °C indicating that cyclization and aromatization reactions of condensed products are taking place in a limited extent. When temperature rises to 600 °C and above, the peak-based selectivity of aromatics such as benzene (7.7 min), toluene (12.9 min), xylene (17.3 min) and styrene (18.3 min), increased drastically from 12% (at 600 °C) to 26.3% (at 800 °C) (for details see Fig. S3).

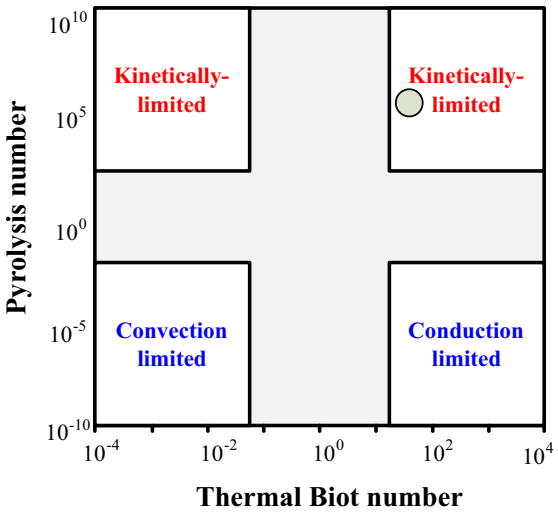

Fig. 3. Thermal mapping of the py-GCMS experiments. λ = 0.16 W/mK, L = 250 μm, h = 2000 W/m^{2}K, ρ (dust rubber) = 529 kg/m^3, Cp = 1417 J/kgK and K (kinetic constant) (s^{-1}) was calculated from the values of Ea and A in Table 2. . Adapted from Paulsen et al. (2013)

These changes in the vapors composition due to the temperature are attributed to secondary reactions occurring in the vapor phase (within solid pores or in homogeneous phase) (Miguel et al., 2006). Therefore, the formation of aromatics during WTs pyrolysis is controlled by transport limitations from particle to vapor phase and/or by the kinetics of the first decomposition step. In fact, Paulsen et al. (2013) propose to identify the transfer/transport mechanisms that controls the process (pure kinetic or thermally controlled regimes) by studying the thermal map of the pyrolysis through the relation between thermal Biot number (for external convection) and the so-called Py- numbers for reaction/-conduction (Py^I) and for reaction/convection (Py^{II}) time scales. Results of the non-dimensional Py^I, Py^{II} and Biot for the present study are placed within the Paulseńs heat transfer map (Fig. 3) and allows identifying that the process is running under kinetic control.

The prevalence of kinetic control could be associated to the short residence time that the first devolatilization/condensation products spends within the reaction zone before they are dragged to the GC analysis. Based on the above-described results, it can be stated that the temperature plays the most important role in the WTs pyrolysis, thus, it defines the product distribution by the kinetics.

3.3.2. Effect of temperature on vapors composition

The pyrolysis temperature have been identified as the most important operation parameter during the WTs pyrolysis (Ding et al., 2015; Miandad et al., 2018; Williams and Besler, 1995; Xu et al., 2018). Here an analysis on the main products deriving from WTs during Py-GC/MS assays is provided, based on the results for peaks area-based selectivity (Eq. (7)).

It is broadly accepted that isoprene and limonene are produced from NR, through a series of β-scission and depropagation reactions of polyisoprene and, by intramolecular cyclization and scission of monomeric isoprene, respectively (Mkhize et al., 2016; Xu et al., 2018). In the present study, the selectivity to limonene continuously decays with the increment of temperature to a minimum of 1.8% at 800 °C, while the isoprene shows two maximums at 500 °C (32%) and 700 °C (36%), respectively (Fig. 4). This decay in the selectivity to limonene is explained by two steps: (I) below 500 °C, limonene transforms into alkenes and (II) from 600 °C a

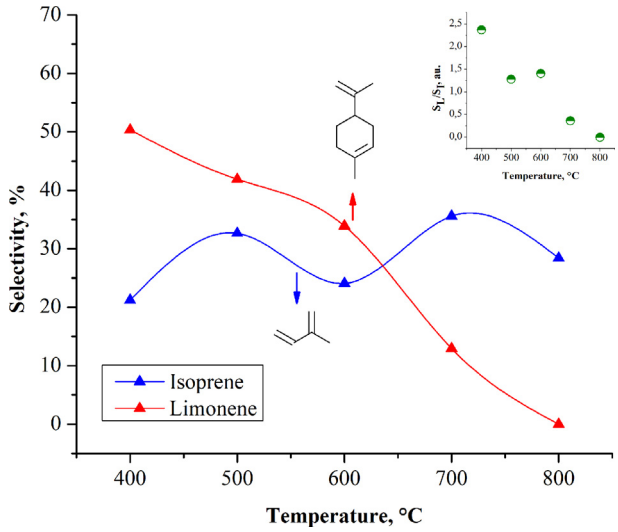

Fig. 4. Effect of pyrolysis temperature on terpenes production from WTs pyrolysis. Py-GC/MS.

portion of the limonene is converted into monocyclic aromatics (xylene, toluene and benzene), respectively.

In fact, limonene can also be produced from isoprene but by the Diels-Alder reaction (coupling of two isoprene monomers) at high temperatures. This was the reason argued by Xu et al. (2018) to explain why they found an increment in limonene formation above 800 °C during their experiments. Moreover, the same molecule (limonene) can decompose in the reverse direction (retro-Diels-Alder) by scission to form isoprene, which could explain the behavior of the isoprene selectivity found here. The selectivity ratios of these two alkenes (insert in Fig. 4, obtained from Eq. (8)) presents a plateau (1.2–1.4 S_L/S_I) between 500 and 600 °C and then it continuously decay to ca. $3.5 * 10^{-4}$ at 800 °C. This suggest that several equilibrated reaction steps could be occurring between isoprene and limonene in the range of 400–700 °C. While, above 700 °C cyclization, hydrogenation and aromatization reactions could be taking place as could be concluded from the increment of monoaromatics selectivity in Fig. 5a. In fact, these reactions were also suggested by Mkhize et al. (2016); Xu et al. (2018) in their pioneering works on WTs pyrolysis mechanisms.

In order to estimate the relative importance of the equilibrated reactions, an approach to equilibrium was estimated for Diels-Alder and cyclization of limonene, respectively. The analysis was performed by implementing a REquil reactor model in Aspen Plus 10.0, considering the above-mentioned reactions and isothermal-isobaric operation. The Polymer-NRTL/Redlich-Kwong equation of state was used for properties estimation. The calculated equilibrium constants were compared to those measured under experimental conditions to calculate the approach to equilibrium (Eq. (9)):

$$A\text{-}t\text{-}E = k_{eq\_exp}/k_{eq\_Model} \quad (9)$$

where i = Diels-Alder, *retro*-Diels-Alder, cyclization; k_{eq_exp} is the equilibrium constant calculated for the experimental data on species composition and k_{eq_Model} is the equilibrium constant estimated by the REquil model.

The small values of A-t-E (0.002 for Diels-Alder and 0.03 for cyclization) at temperatures between 350 and 600 °C, suggests that in this range the reactions are controlled by the kinetics. At temperatures above 650 °C the A-t-E for the retro-Diels-Alder reaction is nearly the unit, which confirms that the reaction is being controlled by the equilibrium.

Yields to aromatics until 700 °C only reached 12.1% which is in very good agreement to that found by Ding et al. (2015), who witnessed a 13.1% at similar conditions. Particularly, in the whole range of temperatures explored, no polyaromatics compounds were detected, which allows inferring that the increase of temperature (particularly above 600 °C) leads to the formation of aromatics by scission and cyclization of limonene and, in less extent, by the de-/hydrogenation of styrene (Xu et al., 2018). The later was also demonstrated by Xu et al. (2018) who found a similar trend during the pyrolysis of waste tires. In fact, the selectivity to toluene, xylene and benzene (BTX) here increases drastically up to 28.7% at 800 °C showing a similar pattern between them (See Fig. 5a). Only the styrene increased and start showing a plateau above 600 °C. The last is attributed to the styrene is formed from styrene-butadiene rubber which is totally converted at 600 °C.

According to Williams and Brindle. (2002), gases form WTs pyrolysis are composed by alkenes, alkanes, H_2, CH_4, CO and CO_2. Nevertheless, identifying the lower molecular weight compounds by Py-GC/MS is not feasible. However, the detected gases (Fig. 5b), depicted a pattern that allows inferring that macromolecules undergoes cracking reactions (specially at high temperatures) to form lower molecular weight hydrocarbons. The maximum %Selectivity for gases was 23% at 800 °C.

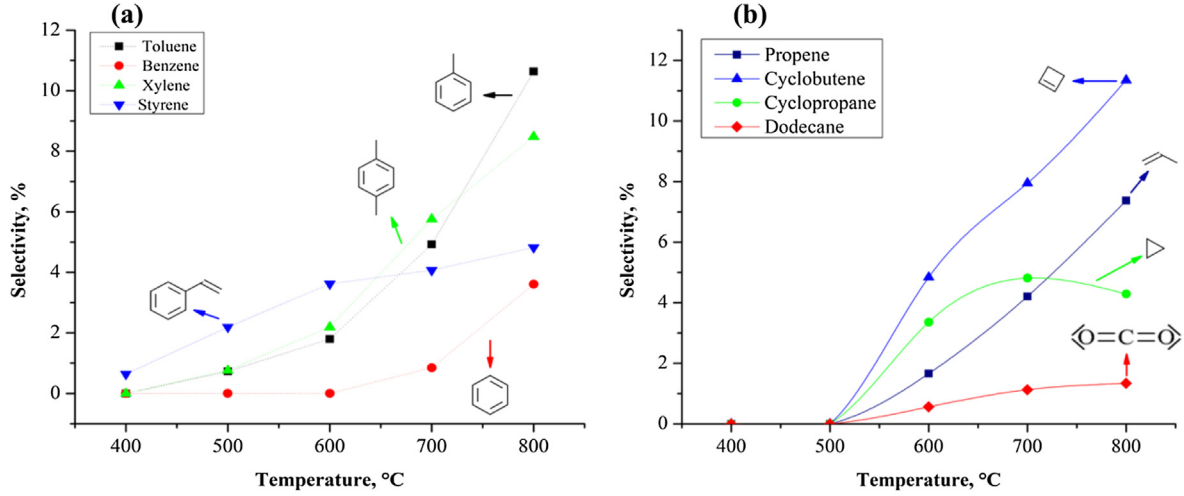

Fig. 5. Effect of pyrolysis temperature on (a) aromatics and (b) gases production from WTs pyrolysis. Py-GC/MS.

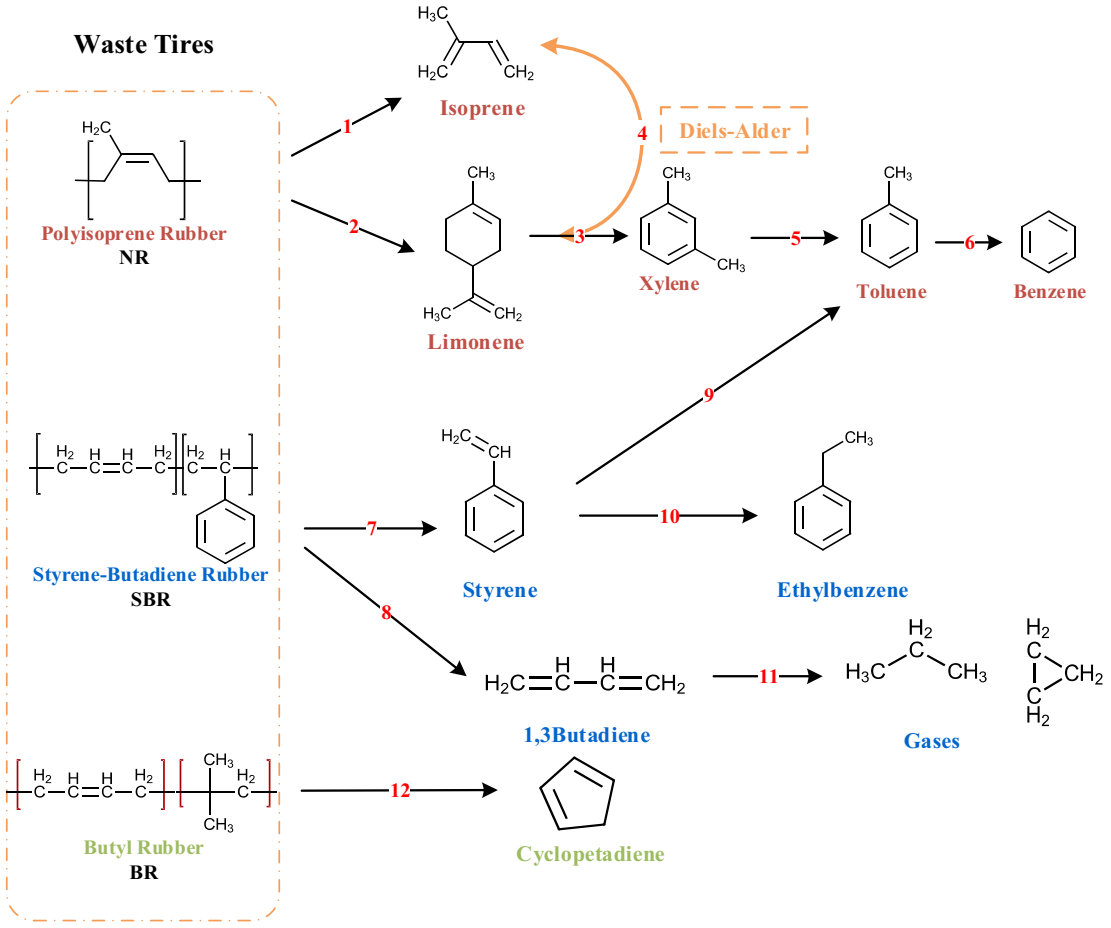

Fig. 6. Mechanistic description of WTs based on TGA-Py-GC/MS observations.

3.3.3. Mechanistic description

The works of Mkhize et al. (2016); Xu et al. (2018) were used as reference to propose a simplified reaction map (Fig. 6) for the WTs pyrolysis, based on the TGA and Py-GC/MS observations. This scheme includes the retro Diels-Alder reaction as an equilibrium step leading to the formation of limonene-isoprene:

The above presented mechanism is in compliance with the experimental observations; nevertheless it is hard to state that this is a general rule, because the reaction routes for WTs pyrolysis are highly sensitive to the material composition, particle sizes, thermal regime (heat transfer or kinetic control) and, thus, to the experimental system.

4. Practical implications of this study

Although, this work is a contribution to the understanding of WTs pyrolysis, still there are several remaining questions. For example, the results obtained at analytical scale must be corroborated at higher scale, in order to take samples for products characterizations and for the validation of the kinetic models and reaction map. This way, the yields of the pyrolytic fractions can be estimated and correlated to the kinetic data to further scaling up the process. Moreover, the effect of catalysts on products distribution and kinetic modelling must be assessed as a way for controlling selectivity to desirable fractions (particularly in oil).

The proposed reaction map and the effects of the pyrolysis temperature explained here, can be used as starting point for future studies, more focused on process design. However, further research is required if process scale up is intended. For example, working at higher scale needs for studying transport limitations, alternatives for feeding systems (considering fines and granules), gas re-utilization strategies (i.e., thermal integration), oil fractionation, etc.

5. Conclusions

Integration of TGA, Py-GC/MS and modelling allows understanding the reaction pathways controlling the WTs pyrolysis and, are the basis for estimating accurate kinetic parameters. At temperatures below 500 °C, isoprene and limonene were the major compounds detected (max. selectivity 71%). At temperatures above 600 °C, the formation of monoaromatics and gases was favored, while limonene and isoprene compositions were ruled by the equilibrated Diels-Alder reaction. At high temperatures limonene undergoes cyclization and the selectivity to benzene, toluene and xylene reached 28.7% (at 800 °C). The kinetic parameters determined by model-based and isoconversional methods were in good agreement (101–176 kJ/mol), presumably due to the experiments were performed under kinetic control. Finally, a simplified reaction map for WTs pyrolysis was proposed to explain the changes caused by the temperature in products composition.

Declaration of Competing Interest

The authors declared that there is no conflict of interest.

Acknowledgements

This work has been financially supported by the project FONDECYT 1190063, FONDECYT 31900610 and CONICYT-PIA/AFB

170007. Authors would like to acknowledge Karen Aravena from CarboCat for the support during TGA analyses.

Appendix A. Supplementary data

Supplementary data to this article can be found online at https://doi.org/10.1016/j.wasman.2019.10.027.

References

Akkouche, N., Balistrou, M., Loubar, K., Awad, S., Tazerout, M., 2017. Heating rate effects on pyrolytic vapors from scrap truck tires. J. Anal. Appl. Pyrolysis 123, 419–429.

Arabiourrutia, M., Lopez, G., Aguado, R., Bilbao, J., Olazar, M., 2019. Coupling gas flow pattern and kinetics for tyre pyrolysis modelling. Chem. Eng. Sci. 201, 362–372.

Arabiourrutia, M., Lopez, G., Elordi, G., Olazar, M., Aguado, R., Bilbao, J., 2007. Product distribution obtained in the pyrolysis of tyres in a conical spouted bed reactor. Chem. Eng. Sci. 62, 5271–5275.

Carrier, M., Windt, M., Ziegler, B., Appelt, J., Saake, B., Meier, D., Bridgwater, A., 2017. Quantitative Insights into the Fast Pyrolysis of Extracted Cellulose, Hemicelluloses, and Lignin. ChemSusChem 10, 3212–3224.

Chen, R., Lun, L., Cong, K., Li, Q., Zhang, Y., 2019. Insights into pyrolysis and co-pyrolysis of tobacco stalk and scrap tire: Thermochemical behaviors, kinetics, and evolved gas analysis. Energy 183, 25–34.

Cheung, K.Y., Lee, K.L., Lam, K.L., Lee, C.W., Hui, C.W., 2011. Integrated kinetics and heat flow modelling to optimise waste tyre pyrolysis at different heating rates. Fuel Process. Technol. 92, 856–863.

Danon, B., Gorgens, J., 2015. Determining rubber composition of waste tyres using devolatilisation kinetics. Thermochim. Acta 621, 56–60.

Danon, B., Mkhize, N.M., Van Der Gryp, P., Görgens, J.F., 2015. Combined model-free and model-based devolatilisation kinetics of tyre rubbers. Thermochim. Acta 601, 45–53.

Dimpe, K.M., Ngila, J.C., Nomngongo, P.N., 2018. Preparation and application of a tyre-based activated carbon solid phase extraction of heavy metals in wastewater samples. Phys. Chem. Earth 105, 161–169.

Ding, K., Zhong, Z., Zhang, B., Song, Z., Qian, X., 2015. Pyrolysis characteristics of waste tire in an analytical pyrolyzer coupled with gas chromatography/mass spectrometry. Energy Fuels 29, 3181–3187.

Ding, K., Zhong, Z., Zhang, B., Wang, J., Min, A., Ruan, R., 2016. Catalytic pyrolysis of waste tire to produce valuable aromatic hydrocarbons: an analytical Py-GC/MS study. J. Anal. Appl. Pyrolysis 122, 55–63.

Han, J., Li, W., Liu, D., Qin, L., Chen, W., Xing, F., 2018. Pyrolysis characteristic and mechanism of waste tyre: a thermogravimetry-mass spectrometry analysis. J. Anal. Appl. Pyrolysis 129, 1–5.

Han, J., Yao, X., Zhan, Y., Oh, S.Y., Kim, L.H., Kim, H.J., 2017. A method for estimating higher heating value of biomass-plastic fuel. J. Energy Inst. 90, 331–335.

Hassan, S.S., Williams, G.A., Jaiswal, A.K., 2019. Moving towards the second generation of lignocellulosic biorefineries in the EU: Drivers, challenges, and opportunities. Renew. Sustain. Energy Rev. 101, 590–599.

Khan, A., Akhtar, J., Shahzad, K., Sheikh, N., Munir, S., 2017. Co-pyrolysis and hyrdogenation of waste tires and thar coal blends. Energy sources, Part A recover. Util. Environ. Eff. 39, 1664–1670.

Khiari, B., Kordoghli, S., Mihoubi, D., Zagrouba, F., Tazerout, M., 2018. Modeling kinetics and transport phenomena during multi-stage tire wastes pyrolysis using Comsol®. Waste Manag. 78, 337–345.

Kim, S., Park, J.K., Chun, H.-D., 1995. Pyrolysis kinetics of scrap tire rubbers. I: using DTG and TGA. J. Environ. Eng. 121, 507–514.

Leung, D.Y.C., Wang, C.L., 1999. Kinetic modeling of scrap tire pyrolysis. Energy Fuels 13, 421–427.

Li, W., Huang, C., Li, D., Huo, P., Wang, Mingfeng, Han, L., Chen, G., Li, H., Li, X., Wang, Y., Wang, Mengyan, 2016. Derived oil production by catalytic pyrolysis of scrap tires. Chinese J. Catal. 37, 526–532.

Lo Presti, D., 2013. Recycled Tyre Rubber Modified Bitumens for road asphalt mixtures: a literature review. Constr. Build. Mater. 49, 863–881.

Martínez, J.D., Cardona-Uribe, N., Murillo, R., García, T., López, J.M., 2019. Carbon black recovery from waste tire pyrolysis by demineralization: Production and application in rubber compounding. Waste Manage. 85, 574–584.

Martínez, J.D., Puy, N., Murillo, R., García, T., Navarro, M.V., Mastral, A.M., 2013. Waste tyre pyrolysis – a review. Renew. Sustain. Energy Rev. 23, 179–213.

Miandad, R., Barakat, M.A., Rehan, M., Aburiazaiza, A.S., Gardy, J., Nizami, A.S., 2018. Effect of advanced catalysts on tire waste pyrolysis oil. Process Saf. Environ. Prot. 116, 542–552.

Miguel, G.S., Aguado, J., Serrano, D.P., Escola, J.M., 2006. Thermal and catalytic conversion of used tyre rubber and its polymeric constituents using Py-GC/MS. Appl. Catal. B Environ. 64, 209–219.

Miranda, R.C., Segovia, C.C., Sosa, C.A., 2006. Pirólisis de llantas usadas: estudio cinético. Ingenierías 32, 8–16.

Mkhize, N.M., van der Gryp, P., Danon, B., Görgens, J.F., 2016. Effect of temperature and heating rate on limonene production from waste tyre pyrolysis. J. Anal. Appl. Pyrolysis 120, 314–320.

Nunes, A.T., dos Santos, R.E., Pereira, J.S., Barbosa, R., Ambrosio, J.D., 2018. Characterization of waste tire rubber devulcanized in twin-screw extruder with thermoplastics. Prog. Rubber Plast. Recycl. Technol. 34, 143–157.

Oboirien, B.O., North, B.C., 2017. A review of waste tyre gasification. J. Environ. Chem. Eng. 5, 5169–5178.

Oyedun, A., Lam, K.L., Fittkau, M., Hui, C.W., 2012. Optimisation of particle size in waste tyre pyrolysis. Fuel 95, 417–424.

Palmeros Parada, M., Osseweijer, P., Posada Duque, J.A., 2017. Sustainable biorefineries, an analysis of practices for incorporating sustainability in biorefinery design. Ind. Crops Prod. 106, 105–123.

Paulsen, A.D., Mettler, M.S., Dauenhauer, P.J., 2013. The role of sample dimension and temperature in cellulose pyrolysis. Energy Fuels 27, 2126–2134.

Portal, M., 2019. Nueva ley obliga a la minería a reciclar 100% de sus residuos de neumáticos [WWW Document]. URL <http://www.portalminero.com/pages/viewpage.action?pageId=159909955>.

Seidelt, S., Müller-Hagedorn, M., Bockhorn, H., 2006. Description of tire pyrolysis by thermal degradation behaviour of main components. J. Anal. Appl. Pyrolysis 75, 11–18.

Senneca, O., Salatino, P., Chirone, R., 1999. Fast heating-rate thermogravimetric study of the pyrolysis of scrap tyres. Fuel 78, 1575–1581.

Singh, S., Nimmo, W., Gibbs, B.M., Williams, P.T., 2009. Waste tyre rubber as a secondary fuel for power plants. Fuel 88, 2473–2480.

Starink, M., 2003. The determination of activation energy from linear heating rate experiments: a comparison of the accuracy of isoconversion methods. Thermochim. Acta 404, 163–176.

Starink, M.J., 1996. A new method for the derivation of activation energies from experiments performed at constant heating rate. Thermochim. Acta 288, 97–104.

Trubetskaya, A., Kling, J., Ershag, O., Attard, T.M., Schröder, E., 2019. Removal of phenol and chlorine from wastewater using steam activated biomass soot and tire carbon black. J. Hazard. Mater. 365, 846–856.

Ucar, S., Karagoz, S., Ozkan, A.R., Yanik, J., 2005. Evaluation of two different scrap tires as hydrocarbon source by pyrolysis. Fuel 84, 1884–1892.

Wall, M., 2019. Automotive industry outlook: managing volatility and leveraging opportunities in a dynamic market environment. © 2019 IHS Markit. All Rights Reserved.

Wei, X., Zhong, H., Yang, Q., Yao, E., Zhang, Y., Zou, H., 2019. Studying the mechanisms of natural rubber pyrolysis gas generation using RMD simulations and TG-FTIR experiments. Energy Convers. Manag. 189, 143–152.

Williams, P.T., Besler, S., 1995. Pyrolysis- thermogravimetric analysis of tires. Fuel 74, 1277–1283.

Williams, P.T., Brindle, A.J., 2002. Catalytic pyrolysis of tyres: Influence of catalyst temperature. Fuel 81, 2425–2434.

Xu, F., Wang, B., Yang, D., Ming, X., Jiang, Y., Hao, J., Qiao, Y., Tian, Y., 2018. TG-FTIR and Py-GC/MS study on pyrolysis mechanism and products distribution of waste bicycle tire. Energy Convers. Manag. 175, 288–297.

Zhang, X., Wang, T., Ma, L., Chang, J., 2008. Vacuum pyrolysis of waste tires with basic additives. Waste Manage. 28, 2301–2310.